

# Efficient CNN Inference on Ultra-Low-Power MCUs via Saturation-Aware Convolution

Shiming Li

Uppsala University  
Sweden  
shiming.li@it.uu.se

Luca Mottola

Politecnico di Milano, RISE, Uppsala University  
Italy and Sweden  
luca.mottola@polimi.it

Yuan Yao

Uppsala University  
Sweden  
yuan.yao@it.uu.se

Stefanos Kaxiras

Uppsala University  
Sweden  
stefanos.kaxiras@it.uu.se

**Abstract**—Deploying lightweight CNN inference tasks on ultra-low-power MCUs is often not limited by space constraint, thanks to the compact size of models, yet inference latency is crucial for preserving energy. We reveal that quantized CNN inference on ultra-low-power MCUs executes unnecessary computations in neurons that produce saturated output values: often times, these neurons still produce the correct output value without fully completing the computation, since the neuron value is too extreme and is eventually systematically clamped at the boundaries allowed by the neuron. We show that with carefully designed condition checks, it is possible to identify and skip these unnecessary computations *without impacting the neuron output*. Based on this, we present *saturation-aware convolution*: an inference technique whereby computations in convolution kernels are executed in an altered order to induce earlier saturation, and saturation checks are inserted to omit unnecessary computations. We integrate our implementation into MCUNet’s TinyEngine, the state-of-the-art neural network code generation and inference framework, and conduct experiments on a Cortex-M0+ MCU. The result based on 7 open-source CNN models displays up to 24% inference time saving, with strictly zero impact on neural network accuracy.

## I. INTRODUCTION

The power-efficient nature of ultra-low-power microcontrollers (MCUs) enables their deployment under extremely power-scarce environments [1, 2]. The rise of TinyML empowers complex data processing on these devices on the network edge, bringing better reliability, energy saving and privacy preservation compared to funneling raw data to the cloud [3].

TinyML models often come with a compact size to fit the limited memory of target platforms. For example, human activity recognition (HAR) [4] classifies human activities through accelerometer data with a convolutional neural network (CNN) of merely 76 kB [5], which is further reduced to 7 kB after quantization and compression into TensorFlow Lite format. In comparison, ultra-low-power MCU can have up to 512 kB program memory [6].

CNNs are not limited by space constraint even on ultra-low-power MCUs. However, inference latency is crucial for energy preservation. Indeed, as these MCUs mostly lack features such as DVFS [7, 8], energy consumption is nearly proportional to their active time [9], and thus every microsecond saved in inference tasks translates directly into energy saving. This calls for faster CNN inference to enhance ultra-low-power MCUs’ computation capability under extreme power constraint [10].

We present a fundamental insight into CNN inference on ultra-low-power MCUs: *there exist effectless computations*

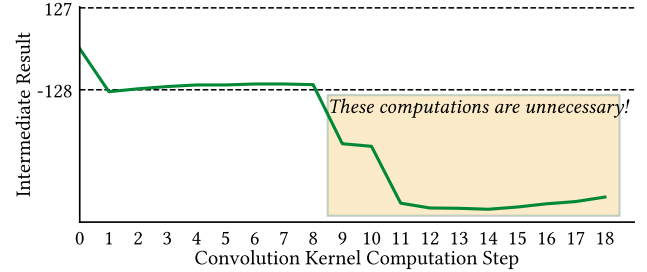


Fig. 1: An example of the computation trace of a convolution operation, where the output neuron’s final value will be saturated to int8. *Because any smaller value will be clamped to -128, removing the last 10 computations from this convolution operation will not change the output neuron’s value.*

when a neuron produces a saturated value. A neuron’s value is determined by a series of computations, such as convolution, based on its input connections, but its actual output value can be saturated, due to boundaries introduced by the output data type’s range, or the activation function. Moreover, even when not crossing the boundaries, a neuron’s output can behave as if eventually saturated, due to a succeeding reduce-max layer. Obviously, in the series of computations that leads to a neuron’s final output value, the neuron value does not always cross the boundaries exactly at the last step. Instead, it is often observed that the intermediate value already goes beyond the boundaries before the end, leaving the final steps of the computation effectless, as the output would be clamped to the same boundary regardlessly.

We exemplify this in Figure 1. The figure depicts the computation trace of a convolution operation for an output neuron in the hand gesture recognition CNN, a lightweight CNN from the STM32 AI Model Zoo [5]. The output neuron’s value is computed through a convolution operation involving 18 input neurons. Since the output is of type int8, the eventual result of the convolution will be clamped to -128. The computation trace reveals that the intermediate computation result has dived below this boundary before all 18 steps finish, and the last 10 steps have no effect on the saturated output value.

This phenomenon is common in CNNs on ultra-low-power MCUs, because they are typically quantized networks in order to account for the lack of hardware floating-point support,

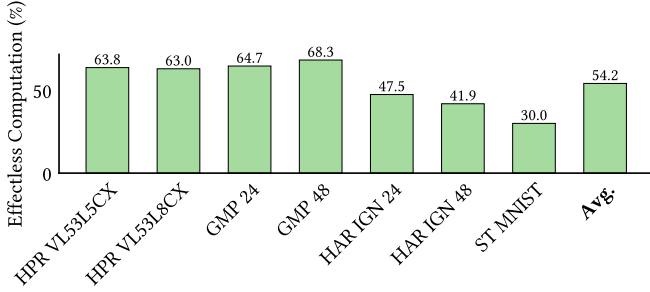


Fig. 2: Pct. of computations with no effect on neuron outputs in convolutional and fully-connected layers in CNN workloads.

where the representable value ranges of the data types are smaller. To win back CNN inference latency, we propose saturation-aware convolution, which executes convolution kernels while dynamically omitting effectless computations without introducing error. Our design expands to three parts:

- *We conceive a solution for zero-error computation omission.* By assuming the most extreme results from any unfinished computation, we only omit the computations upon detecting the final result is bound to be a saturated value. This ensures the output of any neuron value is always correct, even if some computations are omitted from execution.
- *We reorder computations in a convolution kernel to induce earlier saturation.* The altered computation order allows the computation steps with the most impact on the output neuron's value to be executed earlier. This brings more opportunities for omitting computation with zero error.
- *We enable saturation-aware convolution kernel,* by adding extra input to the kernel, which denotes when and how the kernel should pause its execution and check for opportunities to omit remaining computations. This translates effectless computations to practical time savings, and thus energy gains.

We integrate our design into a modified, arm-v6m compatible version of TinyEngine, the code generation and inference engine of the state-of-the-art MCUNet [11]. We conduct experiments on a STM32 development board with a Cortex-M0+ MCU, and observe up to 24% time saving across 7 lightweight CNNs from the open-source MCU neural network suite, STM32 AI Model Zoo [5, 12].

## II. BACKGROUND

### A. CNNs on Ultra-Low-Power MCUs

CNNs on devices on the edge enable more powerful, less communication-intensive, and better privacy-preserving IoT applications [3]. These neural networks come with simple structures, but are capable of complex data processing tasks. For example, Shen et al. deploys a lightweight CNN on drones for water depth estimation with only two to three convolution layers and one fully-connected layer [13]. The HAR network [4, 5] passes accelerometer data through a CNNs of one convolutional layer, one pooling layer and two fully-connected

layers, and recognizes human activity with high accuracy. STMicroelectronics releases a hand posture recognition CNN in their open-source AI Model Zoo [5] with a lightweight structure similar to HAR that recognizes human hand postures from time-of-flight sensor data.

On ultra-low-power MCUs, CNNs are often quantized into 16-bit or even 8-bit integers, since such devices usually lack hardware support for floating point arithmetic. Quantization further eases the space requirements, since less bits are needed to store data. For example, both the HAR CNN and the hand posture CNN reduce to less than 10 kB after quantized with STM32 AI Model Zoo's open-source quantization support [12], while even MSP430 MCUs can have up to 256 kB program memory [14], and some STM32 Cortex-M0+ MCUs come with as much as 512 kB program memory [6].

On the other hand, the inference latency is crucial for MCUs working under restricted power budget. Such devices typically do not support features such as DVFS [7, 8], and their active working power is nearly constant [9]. Reducing inference task latency thus equals reduced active time, hence energy preservation.

### B. Neuron Saturation in Quantized CNNs

The majority of CNNs's inference time is spent on multiply-accumulate operations (MACs). For convolutional layers, the value of an output neuron requires the dot product of a slice of weight matrix that corresponds to the output channel, which we refer to as a convolution kernel, and another array generated by `im2col` transformation from the feature maps. Fully-connected layers, which are essentially a special case of convolutional layers, behave similarly.

The computation in convolutional and fully-connected layers can be described as below:

$$a = \sum_{i=0}^{m-1} x_i \cdot w_i + bias \quad (1)$$

where  $a$  is the accumulation result,  $m$  is the number of computation steps,  $x_i$  are the inputs,  $w_i$  and  $bias$  represent the weights and bias of the kernel, respectively.

For quantized CNNs with integer data types, the accumulation result  $a$  can be larger or smaller than the boundaries that the output neuron allows, which we denote as  $[a_{min}, a_{max}]$ . The output neuron's value is saturated if  $a$  is out of the boundaries. The boundaries may come from:

- *Value range of the output data type.* A multiplication can produce a result with twice the bit as the multipliers. Although the computations in a convolution kernel can use data types with more bits to retain the precision, the output neuron cannot extend its bit width.
- *Activation functions.* For example, the ReLU function [15] limits the minimum value of the output neuron to 0. In quantized CNNs, this boundary will be accordingly quantized and merged with the value range boundary, keeping whichever is tighter.

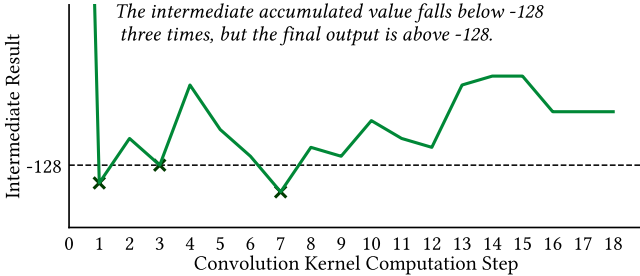


Fig. 3: A counter example in the same layer, but a different neuron as Figure 1. *The intermediate accumulated value going out of bound does not guarantee a saturated final output.*

The above two types of boundaries are static, since they are determined once the training of the model finished. We also identify a third type of boundary, which is dynamically changing as the output neurons in a layer are computed:

- *Boundaries introduced by a succeeding reduce-max layer.* Reduce-max layers eliminate dimensions from a multiple-dimension input, by keeping only the maximum value along one or multiple axes. When the current layer is succeeded by such a layer, the values in previously computed neurons act as a dynamically updating boundary.

We found saturated neurons may contain computations that has no effect, as shown in the example in Figure 1. Our analysis reveals that the effectless computations in saturated neurons of convolutional and fully-connected layers induced by such boundaries can be as much as 68%, as shown in Figure 2. Omitting these computations has the potential of significant energy gains.

There are also existing works that have explored early-exit neural networks [16, 17, 18] which introduces multiple exits to the network structure, anytime ML solutions[7] on energy-constraint devices, or methods that optimize energy efficiency for multiple-exit NNs, such as HaryNet [19] and the network compression scheme by Wu *et al.* [20]. As these works rely on specially designed CNN model or algorithms, we take a different approach: we introduce a new way to execute the inference of the CNN model, allowing for termination inside the convolution kernels, without relying on specific structures in a CNN model.

### III. SATURATION-AWARE CONVOLUTION

We present *saturation-aware convolution*, where a convolution kernel actively tries to identify and omit effectless computations from neurons that generate saturated values, while maintaining the exact same network output. We design a criteria for triggering computation omission, which ensures that the remaining computations are only omitted without introducing computation error when the final output value is certainly saturated. We then propose using computation reordering to expose more opportunities to omit computation. In the end, we explain execution flow of saturation-aware convolution kernels, and introduce a heuristic to efficiently decide when a

convolution kernel should check the intermediate accumulation in attempt to omit computation.

#### A. Omitting Effectless Computations with Zero Error

It is obviously unsafe to terminate the computation for an output neuron in a convolution kernel as soon as the intermediate value falls out of bound. Figure 3 is an example where the convolution operation, despite the intermediate accumulation temporarily falls under  $-128$ , produces a non-saturated value.

We propose a simple solution to this: instead of checking the current accumulated value, we look at *the possible final outputs*. We infer how large or small can the final output be, and compare this with the saturation boundaries. If, for example, at some step even the largest possible final output is below the saturation boundary, then the computation for this output neuron can terminate, and the current intermediate accumulation will lead to the same, correct result.

The most extreme final output can be inferred by assuming each remaining computation step always produces an extreme result. For example, in the case of a int8 CNN, any future input value  $x$  is in  $[-128, 127]$ . Thus, after each computation step  $i$ , knowing the current accumulation  $a_i$ , we assume all remaining computations are produced by  $w$  and  $-128$  or  $127$ , and know  $a_i$ 's future deviation will not exceed  $[d_{min}, d_{max}]$ :

$$d_{min,i} = \sum_{j=i+1}^{m-1} \begin{cases} -128 \cdot w_j, & \text{if } w_j \geq 0 \\ 127 \cdot w_j, & \text{otherwise} \end{cases} + bias \quad (2)$$

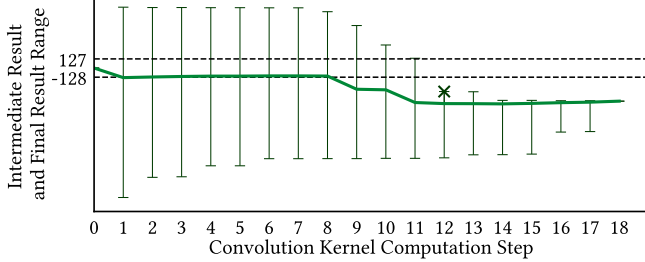
$$d_{max,i} = \sum_{j=i+1}^{m-1} \begin{cases} 127 \cdot w_j, & \text{if } w_j \geq 0 \\ -128 \cdot w_j, & \text{otherwise} \end{cases} + bias \quad (3)$$

We revisit the example in Figure 1. and present it again in Figure 4a. The output neuron's saturation boundaries,  $a_{min}$  and  $a_{max}$ , are  $-128$  and  $127$ , respectively, and the error bars represent  $d_{max}$ 's and  $d_{min}$ 's at each step. At step 12,  $d_{max,12}$  is not enough to pull  $a_{12}$  above  $-128$ , so the remaining computations can be omitted, with 100% certainty that the intermediate  $a_i$  leads to the correct neuron output.

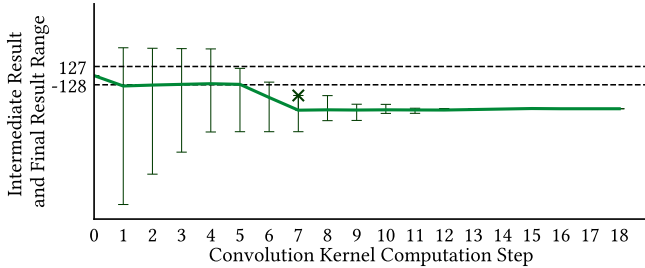
A convolution kernel can practically utilize the information of  $d_{min,i}$  and  $d_{max,i}$  to check whether or not the remaining computations are meaningful. We highlight that all involved values in Equation 2 and 3 are compile-time knowledge. This eases the need for extra computation at run-time, as we can analyze and generate them at compile-time and feed the extra information directly to the convolution kernel.

#### B. Reordering Computations to Induce Earlier Saturation

We notice from Equation 2 and 3 that the values of  $d_{min}$  and  $d_{max}$  are affected by the order of computation in the convolution kernel. We show an example in Figure 4b, which is the same convolution kernel as Figure 4a, but the computations are ordered by the value of  $abs(w)$ . Compared to Figure 4a, the computations involving larger  $w$ 's are first executed, and  $[d_{min}, d_{max}]$  shrinks quicker. Consequently, this example can safely terminate after step 7, much earlier than Figure 4b.



(a) Knowing the maximum possible final accumulated value will be smaller than -128 after step 12, it is safe to terminate the remaining computations here without introducing any error.



(b) The computations in the convolution kernel is reordered by the absolute value of weights. Compared to Figure 4a, the accumulated value stabilizes faster with less divergence. Now the computation can safely terminate at step 7.

Fig. 4: The computation trace of the convolution operation from the same example as Figure 1. The error bars indicate the maximum and minimum possible final accumulated value. This is calculated by assuming all future computations generate the most extreme results allowed by int8.

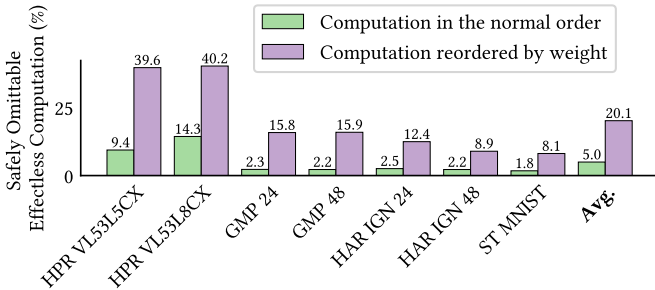


Fig. 5: The percentage of effectual computations that can be omitted with strictly zero error in convolutional and fully-connected layers, with and without computation reordering.

Reordering computations leads to more omitted computations. Intuitively, the optimal computation order is the one that allows the intermediate value of  $a$  to stabilize more quickly [21], leaving less space for deviation in the future. Thus, we propose reordering the computation in a convolution kernel by the absolute value of weight  $w_i$ . The order, however, does not affect the final result of  $a$ , since in a quantized CNNs with integer types, the additions and multiplications are commutative.

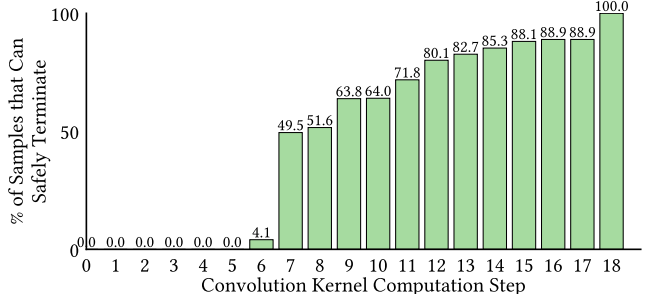


Fig. 6: An example of data obtained from profiling the kernel execution. The data is presented as a cumulative distribution, denoting the probability of triggering safe computation omission for any input to the kernel at each step.

We further present an analysis on 7 workloads involved in our experiments in Figure 5. Reordering the computations in convolution kernels increases the percentage of effectless computations that can be omitted without introducing error by four times, from 5% to 20%.

### C. Selecting Saturation Check Positions via Profiling

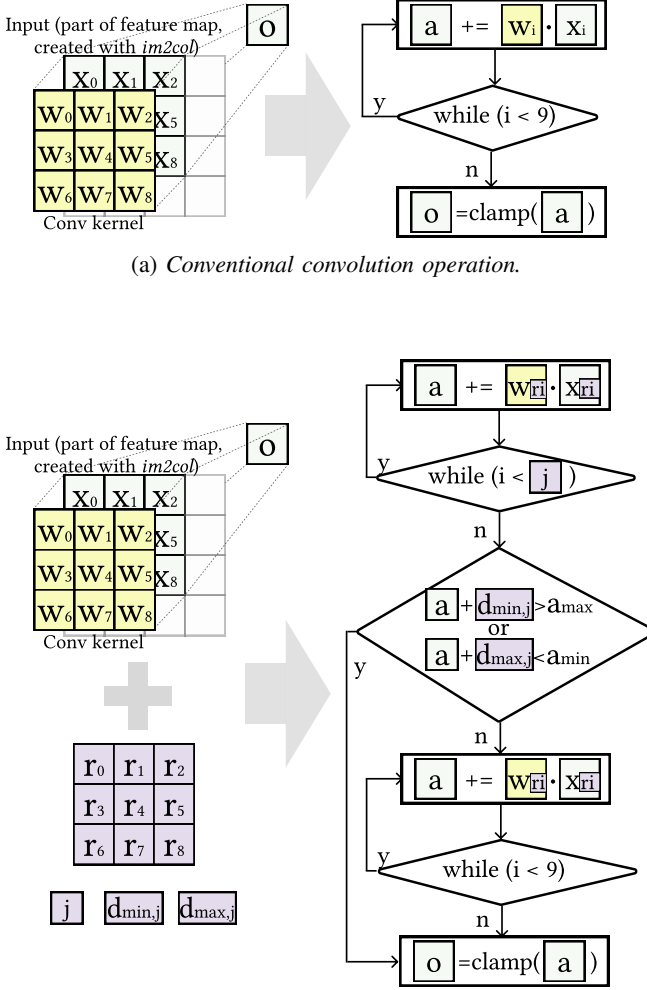
In our design, a convolution kernel periodically executes saturation checks to compare the intermediate accumulation  $a_i$  with  $[d_{min}, d_{max}]$  and  $[a_{min}, a_{max}]$ , and terminate the computation once the final neuron value is bound to be saturated. In practice, it is better to keep the number of saturation checks low for less overhead. Since the opportunity to carry out such checks is limited, when to execute the checks become crucial.

We leave this to be freely configurable, and allow the convolution kernel to accept extra parameters denoting the positions of the checks, as we find the location with the best performance differ from kernel to kernel. We hereby provide a simple heuristic for choosing the check locations, which proves to be effective in our evaluations.

Our heuristic uses compile-time profiling to find the statistically best locations to execute saturation checks. Figure 6 shows a concrete example of profiled data from a filter in the hand posture recognition CNN. To generate the figure, some sample inputs are fed into the network, and for each convolution kernel, we count at each step  $i$  how many times the intermediate value  $a_i$  exceeds the range  $[a_{min} - d_{max,i}, a_{max} - d_{min,i}]$ , marking the point where all the remaining computations can be omitted without introducing error. This data is then transformed into a cumulative distribution shown in this figure.

We find inserting 2 checks in each computation kernel usually delivers satisfactory time saving without introducing significant overhead. The optimal choice can be found by sweeping all the possible combinations of check locations. In this example, step 7 and 12 would be best position, as they together are expected to omit  $(18 - 7) * 49.5\% + (18 - 12) * (80.1\% - 49.5\%) = 7.3$  computation steps.

We highlight that all the data gathered in profiling is platform-agnostic. The profiling do not rely on the target platform, and can be done by compiling and running the neural network and profiling tool on a desktop computer.



(b) *Saturation-aware convolution. The redirection array and the termination check information (in purple color) are fed into the convolution process. The convolution executes in the order of  $r_i$ , and a branch is executed after the  $j$ -th step to check for potential termination.*

Fig. 7: Illustration of conventional convolution and saturation-aware convolution.

#### D. Saturation-Aware Convolution Execution Flow

We allow convolution kernels to omit needless computations, by infusing two types of compile-time knowledge into the convolution kernel. We feed the computation order information, as explained in Section III-B, in the format of a redirection array, so that the index  $i$  of the accumulated elements  $w_i$  and  $x_i$  no longer increases in the numerical order, but are guided by the redirection array. Additionally, we feed to the convolution kernel the saturation check information, consisting of the position to execute saturation checks and the corresponding deviation range  $[d_{min,i}, d_{max,i}]$  of the accumulated value, as in Equation 2 and 3 in Section III-A.

In Figure 7, we compare our saturation-aware convolution with conventional convolution when populating the value for a output neuron. As illustrated by Figure 7b, the convolution

filter takes in a redirection array and the saturation check information. The computation order is guided by the redirection array: instead of using the index  $i$  to directly find elements in  $w$  and  $x$ , the kernel now uses  $i$  to find the next redirected index  $r_i$ , and then access  $w[r_i]$  and  $x[r_i]$ . In this example, one saturation check will be carried out, after step  $j$ . Note that multiple saturation checks are also supported with a similar logic. Moreover, the accumulated value's possible deviation is passed to the convolution kernel as pairs  $d_{min}$  and  $d_{max}$ . Each saturation check compares the final accumulated value range  $[a_i + d_{min,i}, a_i + d_{max,i}]$  with the output neuron's allow range  $[a_{min}, a_{max}]$ . The remaining computations are omitted, once the two ranges do not overlap, meaning the final neuron value is bound to be saturated.

#### E. Implementation

We integrate our implementation of saturation-aware convolution functionalities into the state-of-the-art neural network code generation and inference engine for MCUs, TinyEngine, which is part of MCUNet [11]. TinyEngine takes in CNN models in TensorFlow Lite format, i.e., .tflite format, and generate .c code that can be compiled and run on MCUs. As the vanilla TinyEngine only support arm-v7e architecture [22], which is not compatible with the Cortex-m0+ core on our evaluation platform, we modified the original TinyEngine, where the dependence on arm-v7e instructions is removed and replaced with arm-v6m compatible instructions. We use this version as the baseline, and add our implementations upon it.

Our implementation to support saturation-awareness includes:

- *A model analysis tool*, to populate computation order and the saturation check's boundary conditions by analyzing a convolution kernel's weight and other related parameters.
- *Extension to TinyEngine's code generation tool*, to enable analyzing given models and find layers that benefit from saturation-awareness, and generating CNN inference code and parameters for saturation-awareness support. Similar to the original TinyEngine, fully-connected layers are treated as a special case of convolution with input size of  $1 \times 1 \times n$ .
- *Extension to TinyEngine's kernel functions*, to implement the saturation-aware convolution functionality. Similar to TinyEngine, kernels are optimized by unrolling according to different parameters. For example, we optimize accordingly for saturation-aware convolution with 1, 2 or undetermined number of saturation checks. The code generation logic then picks the best fitting kernel.

Additionally, to support selecting the saturation check positions via compile-time profiling as discussed in Section III-C, we implement tools to automate the compile-time profiling process and corresponding kernel functions that produces profiling data, as well as associated support for the processing of the profiling result.

## IV. EVALUATION

We evaluate CNN model inference speed and energy consumption with and without saturation-aware convolution. We

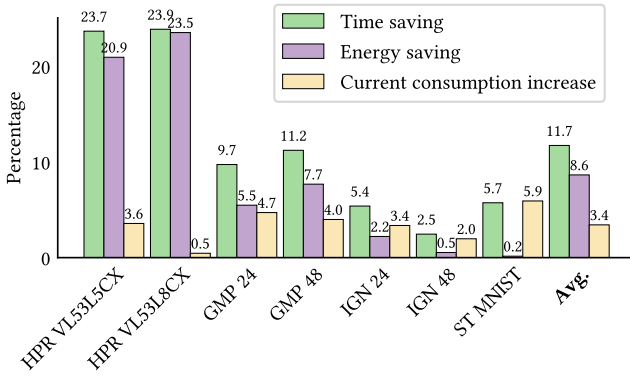


Fig. 8: Inference latency reduction, current consumption increase and energy saving.

conduct experiments on the STM32 NUCLEO-G0B1RE development board, equipped with a Cortex-M0+ MCU. The execution time is measured with `HAL_GetTick()` function. The board's current consumption is measured with Nordic Power Profiler Kit II, which provide stable voltage and collects current measurements with a sample rate of 10kHz, and 100nA resolution via direct pin connections. The average current is then used to estimate the energy consumption together with the average execution time for each workload.

For our saturation-aware code, we use the heuristics explained in Section III-D to decide the positions to execute saturation checks in each kernel. Note that the sample inputs involved in profiling are not reused in our evaluation.

**Workloads.** We evaluate with open-source CNN workloads from the STM32AI Model Zoo Suite [5, 12]. Models in `.h5` type are quantized and compressed into `.tflite` type with STMicroelectronic's quantization support that comes along with the model zoo [12]. The models involved in our evaluation include:

- **ST hand posture recognition CNN (HPR).** This model classifies hand gesture with time-of-flight sensor data. Note that it comes with two variations, one trained with the VL53L5CX, and one with the VL53L8CX sensor.
- **The Ignatov HAR CNN (HAR IGN).** This lightweight model is based on the model proposed by Ignatov [4], and classifies human activity from accelerometer data. It comes with two variations, with an input window length of 24 and 48, respectively.
- **ST global max-pooling HAR CNN (GMP).** Similar to the HAR IGN model, this model also aims at HAR, but uses a different structure consisting of convolution layers and a reduce-max layer. This model also has two variations with different input window lengths.
- **ST MNIST CNN.** This is a image classification model that classifies handwritten digits and letters from the EMNIST dataset [23], with a structure consisting of convolutional and depthwise-convolutional layers similar to Mobilenet [24], but with less layers.

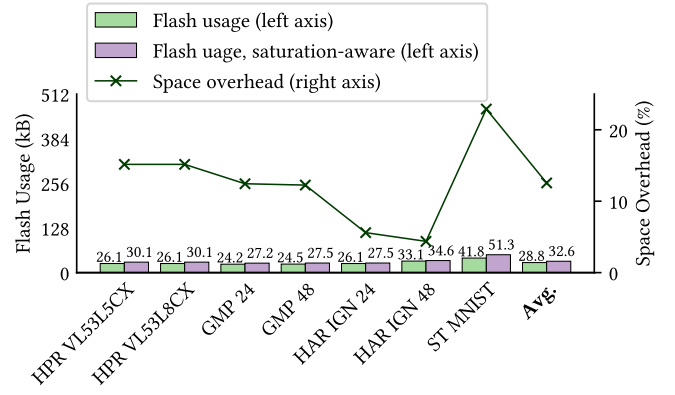


Fig. 9: Flash usage and space overhead in percentage.

**Results.** Saturation-aware convolution effectively reduces inference latency and gains energy saving. We display the time and energy saving in Figure 8. We achieve *up to* 23.9% time saving, and up to 23.5% energy saving on HPR VL53L8CX, averaging 11.7% and 8.6%, respectively, across all workloads.

The current draw on MCUs is primarily determined by the clock frequency [9]. We observe a small increase in current consumption with saturation-aware convolution. This is due to the increased memory access to the redirection array, which is introduced in Section III-B. The increase of current, however, is only 3.6% on average, as in Figure 8 (yellow bar).

We report in Figure 9 the flash usage and space overhead, which is the increase in the flash space usage. All the CNNs are well within the space constraint of the MCU. The increase in flash space used is small; we observe on average only 13% space overhead. The space cost mainly comes from the redirection arrays, as illustrated in Figure 7. The extra information for saturation checks are not significant in size, as we limit the number of checks in each kernel.

We examine the correctness of the inference. We compare the CNNs's outputs for each single experiment with the baseline, and verify that our technique introduces *strictly zero error* to the CNNs and produces the exact same network output.

## V. CONCLUSION

We reveal effectless computations in quantized CNNs on MCUs, in neurons where the computations on the input connections generate a value that is out of the boundaries that the neuron allows, and execution time is spent on computations bearing no effect on the final result after the output neuron value is bound to be saturated. We find such phenomenon to be common on CNNs on ultra-low-power MCUs, since the deployed networks are often quantized into integer types with tighter value ranges on these devices. We present saturation-aware convolution, where a convolution kernel executes the computations in an altered order to induce saturation and predict saturation dynamically via infused compile-time information. The kernels can skip computations with zero error, by always assuming the omitted computations will generate the

most extreme result. Based on experiments involving 7 MCU CNN workloads, our technique shows up to 24% inference latency reduction and up to 23.5% energy saving, with zero impact on network accuracy.

## REFERENCES

- [1] N. A. Bhatti, M. H. Alizai, A. A. Syed, and L. Mottola, “Energy harvesting and wireless transfer in sensor network applications: Concepts and experiences,” *ACM Trans. Sen. Netw.*, vol. 12, Aug. 2016.
- [2] S. Ahmed, B. Islam, K. S. Yildirim, M. Zimmerling, P. Pawelczak, M. H. Alizai, B. Lucia, L. Mottola, J. Sorber, and J. Hester, “The internet of batteryless things,” *Commun. ACM*, vol. 67, pp. 64–73, Feb. 2024.
- [3] N. Schizas, A. Karras, C. Karras, and S. Sioutas, “TinyML for Ultra-Low Power AI and Large Scale IoT Deployments: A Systematic Review,” *Future Internet*, vol. 14, no. 12, pp. 1–45, 2022.
- [4] A. Ignatov, “Real-time human activity recognition from accelerometer data using convolutional neural networks,” *Applied Soft Computing*, vol. 62, pp. 915–922, 2018.
- [5] STMicroelectronics, “STM32 AI Model Zoo,” <https://github.com/STMicroelectronics/stm32ai-modelzoo>, 2023. Accessed on August 20, 2025.
- [6] STMicroelectronics, “STM32G0B1RE,” <https://www.st.com/en/microcontrollers-microprocessors/stm32g0b1re.html>, 2025. Accessed on August 20, 2025.
- [7] S. Ahmed, A. Bakar, N. A. Bhatti, M. H. Alizai, J. H. Siddiqui, and L. Mottola, “The betrayal of constant power  $\times$  time: Finding the missing joules of transiently-powered computers,” in *Proceedings of the 20th ACM SIGPLAN/SIGBED International Conference on Languages, Compilers, and Tools for Embedded Systems*, pp. 97–109, 2019.
- [8] S. Ahmed, A. Qurat, J. Siddiqui, L. Mottola, *et al.*, “Intermittent computing with dynamic voltage and frequency scaling,” in *Proceedings of the 2020 International Conference on Embedded Wireless Systems and Networks*, pp. 1–12, Junction Publishing, 2020.
- [9] STMicroelectronics, “How to Optimize Power Consumption on STM32 MCUs (AN4777).” <https://www.st.com/resource/en/application-note/an4777-how-to-optimize-power-consumption-on-stm32-mcus-stmicroelectronics.pdf>, 2016. Accessed on August 4, 2025.
- [10] H. R. Mendis, K. S. Yıldırım, M. Zimmerling, L. Mottola, and P.-C. Hsiu, “Special session-intermittent tinyml: Powering sustainable deep intelligence without batteries,” in *ACM SIGBED International Conference on Embedded Software (EMSOFT)*, 2025.
- [11] J. Lin, W.-M. Chen, Y. Lin, C. Gan, S. Han, *et al.*, “Mcunet: Tiny deep learning on iot devices,” *Advances in neural information processing systems*, vol. 33, pp. 11711–11722, 2020.
- [12] STMicroelectronics, “STM32 Model Zoo Services.” <https://github.com/STMicroelectronics/stm32ai-modelzoo-services>, 2023. Accessed on August 20, 2025.
- [13] Q. Shen, K. Mahima, K. De Zoysa, L. Mottola, T. Voigt, and M. Flierl, “Cnn-based estimation of water depth from multispectral drone imagery for mosquito control,” in *2023 IEEE International Conference on Image Processing (ICIP)*, pp. 3250–3254, IEEE, 2023.
- [14] Texas Instruments, “MSP430FR5994.” <https://www.ti.com/product/MSP430FR5994>, 2025. Accessed on August 20, 2025.
- [15] A. F. Agarap, “Deep Learning using Rectified Linear Units (ReLU),” *arXiv preprint arXiv:1803.08375*, 2019.
- [16] S. Teerapittayanon, B. McDanel, and H.-T. Kung, “Branchynet: Fast Inference via Early Exiting from Deep Neural Networks,” in *International Conference on Pattern Recognition (ICPR)*, pp. 2464–2469, IEEE, 2016.
- [17] G. Huang, D. Chen, T. Li, F. Wu, L. van der Maaten, and K. Q. Weinberger, “Multi-Scale Dense Networks for Resource Efficient Image Classification,” in *International Conference on Learning Representations (ICLR)*, 2017.
- [18] M. Wołczyk, B. Wójcik, K. Bałazy, I. Podolak, J. Tabor, M. Śmieja, and T. Trzciński, “Zero Time Waste: Recycling Predictions in Early Exit Neural Networks,” *arXiv preprint arXiv:2106.05409*, 2021.
- [19] S. Jeon, Y. Choi, Y. Cho, and H. Cha, “HarvNet: Resource-Optimized Operation of Multi-Exit Deep Neural Networks on Energy Harvesting Devices,” in *International Conference on Mobile Systems, Applications and Services (MobiSys)*, pp. 42–55, 2023.
- [20] Y. Wu, Z. Wang, Z. Jia, Y. Shi, and J. Hu, “Intermittent Inference with Nonuniformly Compressed Multi-Exit Neural Network for Energy Harvesting Powered Devices,” in *ACM/EDAC/IEEE Design Automation Conference (DAC)*, pp. 1–6, 2020.
- [21] F. Bambusi, F. Cerizzi, Y. Lee, and L. Mottola, “The Case for Approximate Intermittent Computing,” in *ACM/IEEE International Conference on Information Processing in Sensor Networks (IPSN)*, pp. 463–476, 2022.
- [22] mit-han-lab, “Github page: tinyengine.” <https://github.com/mit-han-lab/tinyengine>, 2020. Accessed on August 20, 2025.
- [23] G. Cohen, S. Afshar, J. Tapson, and A. Van Schaik, “Emnist: Extending mnist to handwritten letters,” in *2017 international joint conference on neural networks (IJCNN)*, pp. 2921–2926, IEEE, 2017.
- [24] A. G. Howard, M. Zhu, B. Chen, D. Kalenichenko, W. Wang, T. Weyand, M. Andreetto, and H. Adam, “MobileNets: Efficient Convolutional Neural Networks for Mobile Vision Applications,” *arXiv preprint arXiv:1704.04861*, 2017.